

Milky Way simulations: the Galaxy, its stellar halo and its satellites – insights from a hybrid cosmological approach

Gabriella De Lucia*

INAF - Astronomical Observatory of Trieste, via G.B. Tiepolo 11, I-34143 Trieste, Italy

Received 2012, accepted 2012

Published online later

Key words Galaxy: formation – Galaxy: evolution – Galaxy: halo – Galaxy: abundances

Our ‘home galaxy’ - the Milky Way - is a fairly large spiral galaxy, prototype of the most common morphological class in the local Universe. Although being only *a galaxy*, it is the only one that can be studied in unique detail: for the Milky Way and for a number of members of the Local Group, a wealth of observational data is available about the ages and chemical abundances of their stars. Much more information is expected to come in the next few years, from ongoing and planned spectroscopic and astrometric surveys, providing a unique benchmark for modern theories of galaxy formation. In this review, I will summarize recent results on the formation of our Milky Way, its stellar halo, and its satellite galaxies. I will focus, in particular, on results obtained in the framework of hybrid models of galaxy formation, and refer to other reviews in this issue for studies based on hydrodynamical simulations.

© 2012 WILEY-VCH Verlag GmbH & Co. KGaA, Weinheim

1 Introduction

Our Galaxy - the Milky Way - is a fairly large spiral galaxy consisting of four stellar components: most of the stars are distributed in a thin disk, exhibit a wide range of ages, and are on high angular momentum orbits. About 10–20 per cent of the mass in the thin disk resides in a distinct component which is referred to as the thick disk. This is composed of old stars, that have on average lower metallicity than those of similar age in the thin disk, and are on orbits of lower angular momentum. The Galactic bulge is dominated by an old and relatively metal-rich stellar population, with a tail to low abundances. Finally, a tiny fraction of the total stellar mass (only a few percent) resides in the stellar halo, which is dominated by old and metal poor stars on low angular momentum orbits.

Although the Milky Way is only *one galaxy*, it is our *home galaxy* and, as such, it is the only one that we can study in unique detail. Over the past decades, accurate measurements of physical properties (ages and metallicities) and kinematics have been collected for a significant number of individual stars. Many more data are coming in the next future, from ongoing or planned astrometric and spectroscopic surveys. This wealth of observational data and details provide a unique benchmark for modern theories of galaxy formation and evolution.

Historically, chemical and kinematic information for stars and stellar systems in the solar neighbourhood were used as a basis to formulate the first galaxy formation models. Eggen, Lynden-Bell & Sandage (1962) analysed a sample of ~ 200 dwarfs and showed that stars with the lowest

metallicity tended to move on highly elliptical orbits. The data were interpreted as evidence that the oldest stars in the galaxy were formed out of gas collapsing from the halo onto the plane of the galaxy, on relatively short time-scales (a few times 10^8 years). About one decade later, Searle & Zinn (1978) analysed a sample of ~ 200 giants and ~ 20 globular clusters finding no radial abundance gradients. These observations led to the formulation of a different scenario in which the stellar halo forms through the agglomeration of many sub-galactic fragments, that may be similar to the surviving dwarf spheroidal satellites (dSphs) of our Galaxy.

The Searle & Zinn scenario appears to be in qualitative agreement with expectations from the hierarchical cold dark matter model (CDM), and evidence in support of the proposed picture has mounted significantly over the past years. This ranges from the detection of significant clumpiness in the phase space distribution of halo and disk stars, to the detection of satellite galaxies caught in the act of tidal disruption. Some problems, however, remain. A first one was pointed out by Shetrone, Cote & Sargent (2001) who noted that stars in the Local Group dSphs have lower α abundances than stars in the stellar halo. These observations suggest that the Galactic stellar halo cannot result from the disruption of satellite galaxies similar to the *surviving* dSphs of the Local Group. The difficulty can be overcome if surviving satellites are intrinsically different from satellites that have contributed to the formation of the stellar halo (I will discuss this in more detail in Section 4).

A potentially more serious problem with the Searle & Zinn scenario was pointed out by Helmi et al. (2006) who found a lack of stars of low metallicity in four nearby dSphs (Sculptor, Sextans, Fornax, and Carina), suggesting that the material that gave origin to these galaxies was enriched prior

* e-mail: delucia@oats.inaf.it

to their formation. In addition, Helmi et al. found that the metal-poor tail of the dSph metallicity distribution is significantly different from that of the Galactic halo, arguing that the progenitors of present day dSphs are fundamentally different from the building blocks of our Galaxy, even at earliest epochs. The picture has, however, changed recently as many studies have detected very metal-poor stars both in classical and in ultra-faint dSphs (e.g. Kirby et al 2008; Frebel et al. 2010).

Another element of crisis with respect to the current standard cosmological paradigm is provided by the so called *missing satellite problem*, i.e. the observation that substructures resolved in a galaxy-size DM halo significantly outnumber the satellites observed around the Milky Way (Klypin et al. 1999; Moore et al. 1999). It has long been realized, however, that this problem might have an astrophysical solution. In particular, the presence of a strong photoionizing background, possibly associated with the reionization of the Universe, can suppress accretion and cooling in low-mass haloes thereby suppressing the formation of small galaxies (e.g. Efstathiou 1992, Okamoto, Gao & Theuns 2008 and references therein). Galaxy formation in small haloes can also be significantly suppressed by supernovae driven winds, and the combination of these two physical processes can bring the predicted number of luminous satellites in agreement with observational data (e.g. Kauffmann, White & Guiderdoni 1993; Bullock, Kravtsov & Weinberg 2000; Benson et al. 2002).

Another potential problem with the satellite galaxies has emerged in more recent years: the dwarf satellite galaxies of the Milky Way span several orders of magnitude in luminosity. Yet, the mass enclosed within a small radius (300 or 600 pc) appears to be roughly constant (Strigari et al. 2008), suggesting the existence of a minimum mass scale which is not present in the primordial CDM power spectrum of density perturbation. Therefore, in the framework of the current favourite cosmological model, such a minimum scale can only result from astrophysical processes.

The discovery of a new population of ultra-faint satellites in the past few years has led to a renewed interest in the physics of dwarf galaxy formation. It should be noted, however, that this discovery did not alleviate the original missing satellite problem, as all the newly discovered satellites are fainter than the classical ones. New impetus to the field has also been given by the completion of extremely high resolution N -body simulations of Milky-Way size haloes (Springel et al. 2008, Diemand et al. 2008).

Space limit does not allow an exhaustive review of all studies related to the formation and evolution of the Milky Way and its satellite population. In the following, I will therefore focus on the most recent results obtained in the framework of *hybrid models of galaxy formation* (see next section). I refer to the reviews by C. Scannapieco and V. Springel for related discussions focused on hydrodynamical simulations.

2 Simulations and Galaxy Formation Models

The formation and the evolution of the baryonic component of galaxies is regulated by a number of non-linear processes operating on vastly different scales (e.g. shocking and cooling of gas, star formation, feedback by supernovae and active galactic nuclei, etc.). Most of these processes are poorly understood, even when viewed in isolation. The difficulties grow significantly when considering that, in the real Universe, these processes act together in a complex network of actions, back-reactions, and self-regulation.

In recent years, different approaches have been used to link the observed properties of luminous galaxies to the dark matter haloes within which they reside. Among these, semi-analytic models have developed into a powerful and widely used tool to study galaxy formation in the framework of the currently standard model for structure formation. In this approach, the evolution of the baryonic component is modelled invoking simple, yet physically and observationally motivated *prescriptions*. These techniques find their seeds in the pioneering work by White & Rees (1978), but have been substantially extended and refined in the last years by a number of different groups (recent work includes De Lucia & Blaizot 2007, Monaco et al. 2007, Somerville et al. 2008, Benson & Bower 2010, Guo et al. 2011).

Modern semi-analytic models of galaxy formation take advantage of high resolution N -body simulations to specify the location and evolution of dark matter haloes - which are assumed to be the birthplaces of luminous galaxies. Using this *hybrid* approach, it is possible not only to predict observable physical properties such as luminosities, metallicities, star formation rates, etc., but also to provide fully dynamically consistent spatial and kinematical information for all model galaxies. This allows more accurate and straightforward comparisons with observational data to be carried out.

Most of the results discussed below are based on N -body re-simulations of ‘Milky-Way’ haloes: first, a cosmological simulation of a large region is used to select a suitable target halo. The particles in this halo and its surroundings are then traced back to their initial Lagrangian region and replaced with a larger number of lower mass particles. Outside the high-resolution region, particles of mass that increases with distance are used, so that the computational effort is concentrated on the region of interest while a faithful representation of the large scale density field is maintained.

In the following, I will present results obtained mainly from two sets of re-simulations. For the GA series (Stoehr et al. 2003), a Milky-Way halo was selected as a relatively isolated halo which suffered its last major merger at $z > 2$, and with approximately the correct peak rotation velocity. The selected halo was then re-simulated at a series of four progressively higher resolution, with the highest resolution simulation (the GA3) using a particle mass $m_p = 2.947 \times 10^5 M_\odot$ and a gravitational softening $\epsilon = 0.18 h^{-1} \text{kpc}$. In the Aquarius project, carried out by the Virgo Consor-

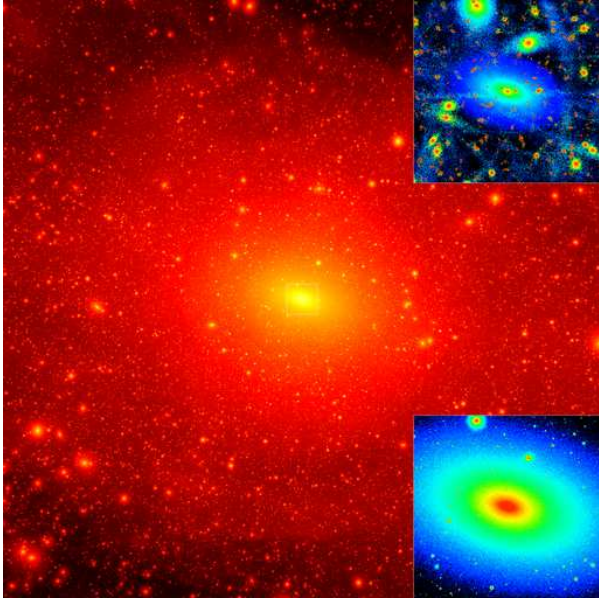


Fig. 1 From Diemand et al. (2008): projected dark matter density-square map of the Via Lactea II simulated halo. The region shown corresponds to a 800 kpc cube. The insets focus on an inner 40 kpc cube, in local density (bottom), and in local phase space density (top).

tium, six galactic dark matter haloes with masses comparable to that of the Milky Way were extracted from a cosmological box and re-simulated at varying levels of resolution (Springel et al. 2008). In the following, I will present results obtained by coupling the second highest level of resolution of the Aquarius haloes (m_p ranges from 6.447×10^3 to $1.399 \times 10^4 M_\odot$, and $\epsilon = 65.8$ pc) with independently developed semi-analytic models. Finally, the Via Lactea II simulation has been recently completed by Diemand et al. (2008). A projected dark matter density map from this simulation is shown in Fig. 1 (this is one galaxy-mass halo, simulated using particles of mass $m_p = 4.1 \times 10^3 M_\odot$, and $\epsilon = 40$ pc).

3 The Galaxy

The formation and evolution of different stellar components of the Milky Way has been studied in detail over the past decades, using a combination of N -body simulations and analytic models. In the framework of cosmological hydrodynamical simulations, the formation of realistic disk galaxies has long been considered, and still largely remains, a challenge. This is due to a combination of numerical effects and limitations of the treatment of baryonic processes. Much progress has been made, highlighting the crucial role played by feedback in preventing overcooling and regulating the assembly of galaxies in order to avoid catastrophic angular momentum losses (see e.g. Scannapieco et al. 2011 and references therein).

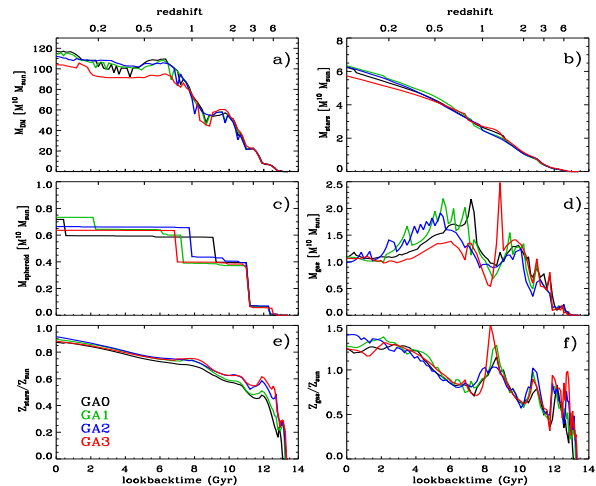


Fig. 2 From De Lucia & Helmi (2008): evolution of the dark matter mass (panel a), total stellar mass (panel b), spheroid mass (panel c), cold gas mass (panel d), stellar metallicity (panel e), and gas metallicity (panel f) for the model Milky Way galaxies in the four simulations of the GA series (lines of different colours).

In the framework of hybrid models of galaxy formation, a recent work has been carried out by De Lucia & Helmi (2008) by taking advantage of the GA series. Figure 2 is reproduced from this work, and shows the evolution of different mass and metallicity components for the model Milky Way galaxies in all four simulations of the series (black corresponds to the lowest resolution simulation, and red to the highest resolution one). The histories are constructed by tracking the evolution of the main progenitor, obtained by linking the galaxy at each time-step to the progenitor with the largest stellar mass. For this model Milky Way, the galaxies merging onto the main branch have stellar masses that are much smaller than the current mass of the main progenitor, over most of the galaxy's life-time, explaining the smooth increase of the stellar mass component (panel b). The mass of the spheroidal (panel c) component grows in discrete steps as a consequence of the assumption that it grows during mergers and disk instability events (see original paper for details). In this particular model, disk instability contributes about half of the final stellar mass in the spheroidal component. Minor mergers contribute to the other half, and all occur at later times with respect to the disk instability episodes.

Interestingly, the model provides consistent evolutions for all four simulations, despite a very large increase in numerical resolution (a factor ~ 800 between GA0 and GA3). Some panels (e.g. panels b, e, and f) do not show convergence of the results. This is driven by the lack of complete convergence in the N -body simulations (panel a shows a clear difference between GA3 and the lower resolution simulations). The reference model used in the work by De Lucia & Helmi is in relatively good agreement with observational

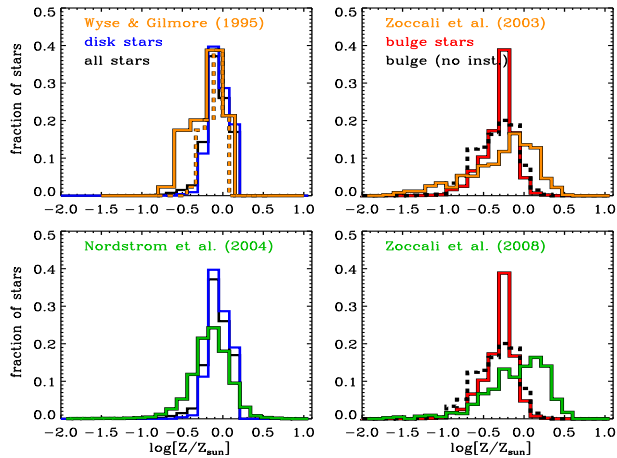


Fig. 3 From De Lucia & Helmi (2008): metallicity distribution for stars in the disk (blue histograms, left panels) and spheroid (red histograms, right panels) of the model Milky Way from the simulation GA3. The solid black histograms in the left panels show the metallicity distribution for all stars in the model galaxy, while the dashed black histograms in the right panels show the metallicity distribution of stars in the spheroidal component in a model with disk instability switched off. Orange and green histograms show different observational measurements.

measurements (but the mass of the spheroid is slightly lower and the gas content higher than the observational estimates).

The metallicity distributions of the stars in the disk and spheroid of the model Milky Way from the simulation GA3 are shown in Fig. 3. The left panels show the metallicity distribution of all stars (black histograms) and of the stars in the disk (blue histograms), compared to different observational measurements. The figure shows that the metallicity distribution of disk stars in the model Milky Way peaks at approximately the same value as observed, but exhibits a deficiency of low metallicity stars. In comparing the model and observed metallicity distributions, two factors should be taken into account: (1) the observational metallicity measurements have some uncertainties (~ 0.2 dex) that broaden the true underlying distribution, and are not included in the theoretical prediction; (2) the metallicity estimate used in the observational studies is an indicator of the *iron* abundance, which is mainly produced by supernovae Ia and not well described by the instantaneous recycling approximation adopted in the model by De Lucia & Helmi. In order to estimate the importance of this second caveat, they have converted the measured $[\text{Fe}/\text{H}]$ into $[\text{O}/\text{H}]$ using a linear relation, obtained by fitting observational data for thin disk stars. The result of this conversion is shown by the dashed orange histogram in the top panel of Fig. 3, and is much closer to the modelled $\log[Z/Z_{\odot}]$ distribution.

The right panels in Fig. 3 show the metallicity distribution of the spheroid stars in the fiducial model (red histogram) and in a model where the disk instability channel

is switched off (dashed black histograms). The metallicity distribution of the model spheroid peaks at lower value than observed, and it contains a fraction of high metallicity stars that is smaller than that observed. Comparison between the solid red histogram and the black dashed histogram shows that disk instability is responsible for the pronounced peak around $\text{Log}[Z/Z_{\odot}] \sim -0.25$, due to the transfer of a large fraction of disk stars into the spheroidal component. The same caveat discussed above applies to the metallicity distribution of the spheroidal component. Note, however, that a conversion from $[\text{Fe}/\text{H}]$ to $[\text{O}/\text{H}]$ of the observed metallicity scale would bring most of the observed bulge stars to $[\text{O}/\text{H}] \gtrsim -0.2$, suggesting that the model spheroid in the work by De Lucia & Helmi is significantly less metal rich than the observed Galactic bulge.

The use of the instantaneous recycling approximation represents clearly one important limitation of the study discussed above. Work is ongoing to relax this approximation and include a more detailed treatment of the chemical enrichment, by taking into account the lifetime of stars of different mass. Detailed chemical models for the Milky Way are available (see e.g. Matteucci 2008 and references therein). Unfortunately, however, these analytic and numerical models are often carried out under the assumption that the galaxy evolved in isolation (the models are not embedded in a cosmological framework), and often assuming ad hoc initial conditions.

4 The stellar halo

As mentioned above, the stellar halo is the Milky Way stellar component that contains the smallest fraction of its stars. Yet, it is arguably the component that carries the most useful information about the evolutionary history of the Galaxy because it contains its most metal-poor stars. The origin and structure of the stellar halo has been studied by several authors, using different techniques (for a review, see Helmi 2008). These include cosmological simulations with and without baryonic physics, and phenomenological models, usually in combination with N -body simulations that provide the dynamical history of the system.

For example, Bullock & Johnston (2005) combined mass accretion histories of galaxy-size haloes, constructed using the extended Press-Schechter formalism, with chemical evolution models for individual satellites. For each accretion event, they run N -body simulations (dark matter only), following the dynamical evolution of the accreted satellites, which are placed on orbits consistent with those found in cosmological simulations. A variable mass-to-light ratio was assigned to each dark matter particle, and chemical evolution was modelled by considering both Type II and Type Ia supernovae. The build up and chemical properties of the stellar halo in these models was analysed by Font et al. (2006). These authors showed that the model reproduces the systematic differences between the chemical abundances of stars in satellite galaxies and those in the Milky Way halo.

In their model, the agreement with the observed trend is a consequence of the fact that the stellar halo originates from a few relatively massive satellites that were accreted early on and were enriched in α elements by type II supernovae. The model surviving satellites are accreted much later, have more extended star formation histories and stellar population enriched to solar level by both type II and type Ia supernovae. In the model by Font et al., the most metal-poor stars are located in the inner 10 kpc, which is in contrast with the trends found by Carollo et al. (2007).

The formation and structure of the stellar halo was studied, in the context of a hybrid model of galaxy formation, in the work by De Lucia & Helmi (2008) mentioned above. The working hypothesis used in this study is that the stellar halo built from the cores of the satellite galaxies that merged with the Milky Way over its lifetime. In order to identify the stars that end up in the stellar halo, the full merger tree of the model Milky Way galaxy was constructed, and the galaxies that merge onto the main branch of the galaxy identified. These galaxies were then traced back until they are for the last time central galaxies, and a fixed fraction (ten per cent in the fiducial model) of the most bound particles of their parent haloes were *tagged* with the stellar metallicity of the galaxies residing at their centre.

Fig. 4 shows the stellar masses (top panel) and metallicities (middle panel) of all galaxies accreted onto the main branch for the simulation GA3, as a function of the lookback time of the galaxy's merger. Stellar masses and metallicities correspond to those at the time of accretion. The solid red lines in these panels show the evolution of the stellar mass and of the stellar metallicity in the main progenitor of the Milky Way galaxy (as in Fig. 2). The bottom panel of Fig. 4 shows the number of particles associated with the dark matter haloes before accretion, again as a function of the merging time of the galaxies that reside at their centre. Red symbols indicate objects belonging to haloes with more than 500 bound particles before accretion. For these objects, both the time of accretion (open symbols) and the merger time (solid symbols; this is given by the dynamical friction timescale) are indicated in the figure. Most of the galaxies that merge onto the main branch have stellar masses and metallicities that are much smaller than the current mass and metallicity of the main progenitor, over most of the galaxy's life-time. Most of the accreted galaxies lie in quite small haloes and only a handful of them are attached to relatively massive systems. These are the galaxies that contribute most to the build-up of the stellar halo. The red symbols in the bottom panel of Fig. 4 show that most haloes with more than ~ 500 particles were all disrupted more than ~ 6 Gyr ago. These haloes contain the few galaxies with stellar mass larger than $10^6 M_{\odot}$ which merge onto the main branch over the galaxy's life-time (top panel). The stellar metallicities are generally relatively low, with a median value of $\sim 0.3 Z_{\odot}$, with larger values associated with larger galaxies (see below).

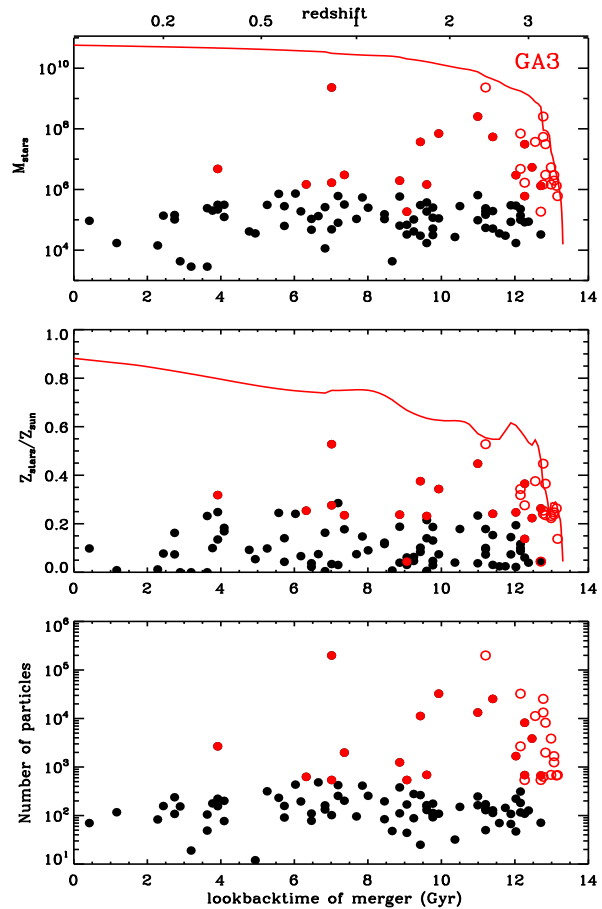


Fig. 4 From De Lucia & Helmi (2008): stellar masses (top panel) and metallicities (middle panel) for all galaxies accreted onto the main branch for the simulation GA3, as a function of the lookback time of the galaxy's merger. The solid red lines in the top and middle panels show the evolution of the stellar mass and metallicity in the main progenitor of the Milky Way. The bottom panel shows the number of particles associated with the dark matter halo at the time of accretion, again as a function of the merging time of the galaxy that is located at its centre. Red symbols indicate objects associated with substructures with more than 500 particles. Red open symbols correspond to red filled circles but are plotted as a function of the time of accretion.

The approach used by De Lucia & Helmi is similar to that adopted by Bullock & Johnston (2005), although the two methods differ in a number of details. Results by Font et al. (2007) are in good agreement with those illustrated in Fig. 4: they find that one or a few more satellites in the range $10^8 - 10^{10} M_{\odot}$ can make up 50-80 per cent of the stellar halo, and that most of them are accreted early on ($t_{\text{accr}} > 9$ Gyr). In agreement with findings by Bullock & Johnston (2005), the halo resulting from the simulations of De Lucia & Helmi (2008) exhibits a steeper profile and is

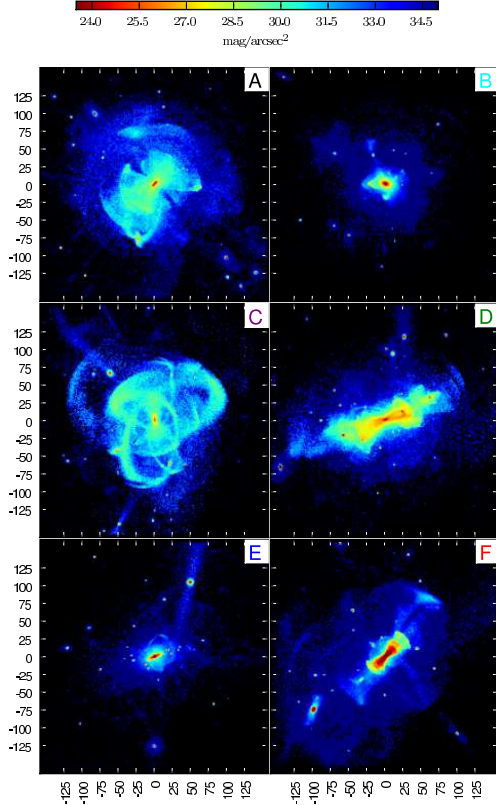


Fig. 5 From Cooper et al. (2010): V -band surface brightness of model stellar haloes (and surviving satellites), to a limiting depth of 35 mag/arcsec^2 . The axis scales are in kiloparsec.

more centrally concentrated than the dark matter profile. In addition, they find that star particles with metallicity larger than $0.4 Z_{\odot}$ are more centrally concentrated than star particles of lower abundances, in qualitative agreement with the measurements by Carollo et al. (2007).

A more sophisticated tagging scheme has been recently used by Cooper et al. (2010) who take advantage of the higher resolution simulations from the Aquarius project. In their study, Cooper et al. assume that the energy distribution of newly formed stars traces that of the dark matter. They then order the particles by binding energy and select some fraction (f_{MB}) of these most bound particles to be tagged. f_{MB} is treated as a free parameter, and is fixed by comparing model predictions with observational measurements of the structure and kinematics of the Milky Way satellites. The tagging scheme adopted by Cooper et al. is similar to that used in De Lucia & Helmi but, again, the details are different: De Lucia & Helmi tag the most bound ten per cent of particles in a satellite, but perform this tagging only once (i.e. at the time when its parent halo becomes a subhalo of the main halo). In contrast, Cooper et al. apply their tagging scheme each time a new stellar population is formed and chose the subset of dark matter particles according to the instantaneous dynamical state of the host halo.

Fig. 5 shows a $300 \times 300 \text{ kpc}$ projected surface brightness map of the stellar halo at $z = 0$, for each of the six Aquarius dark matter haloes. Substantial diversity among the six haloes is apparent. A few haloes (e.g. Aq-B and Aq-E) are characterized by strong central concentrations, while others show extended envelopes out to $75 - 100 \text{ kpc}$. Each envelope is the superposition of streams and shells that are phase-mixed to varying degrees. Most haloes exhibit a strongly prolate distribution of stellar mass, particularly in the inner regions. The brightest and most coherent structures visible in Fig. 5 can be associated with the most recent accretion events. In addition, Cooper et al. show that their model stellar haloes span a wide range of accretion histories, ranging from a gradual accretion of many progenitors (Aq-A, Aq-C and Aq-D) to one or two significant accretions (Aq-B, Aq-E and Aq-F). All the most significant contributors to the stellar haloes were accreted more than 8 Gyr ago, with the exception of Aq-F. For this halo, more than 95 per cent of the halo was contributed by the late merger of an object of stellar mass greater than the SMC infalling at $z \sim 0.7$. Finally, only in two haloes (Aq-C, Aq-D), the stars stripped from the surviving satellites represent the largest fraction (up to ~ 70 per cent) of the stellar halo. In the other haloes, stars stripped from surviving satellite represent less than ~ 10 per cent of the stellar halo.

Fig. 6 shows the spherically averaged density profiles of halo stars for the six haloes analysed in Cooper et al. The density profiles have been obtained by excluding material bound in surviving satellites, but making no distinction between streams, tidal tails or other overdensities. Dark matter haloes are well fitted by the Einasto profiles (shown as dashed lines in the figure - see also Springel et al. 2008), while the stellar haloes exhibit a notable degree of substructures which is due to the contribution of localized and spatially coherent subcomponents within the haloes. The shapes of the density profiles are broadly similar, showing a strong central concentration and an outer decline which is steeper than that of the dark matter halo. Cooper et al. note that the density profile of the many-progenitor haloes (Aq-A, Aq-C and Aq-D) can be fit with broken power-law profiles, with indices similar to the Milky Way ($n \sim 3$) interior to the break. In contrast, two of the few-progenitor haloes (Aq-B and Aq-E) have steeper profiles and show no obvious break, although their densities in the solar shell are comparable to those of the many-progenitor haloes. Aq-F is dominated by a single progenitor, and its debris retains a high degree of unmixed structure at $z = 0$.

In a follow-up study, Cooper et al. (2011) have compared predictions from their models to the two-point correlation function for Galactic halo stars (this is based on a catalogue of blue horizontal branch stars identified in the Sloan Digital Sky Survey). Considering only stars with $r > 20 \text{ kpc}$, five out of the six Aquarius haloes show statistically significant correlation on scales equivalent to $\sim 1-8 \text{ kpc}$, and most of the models are consistent with the observational data for the outer regions ($r > 30 \text{ kpc}$). For

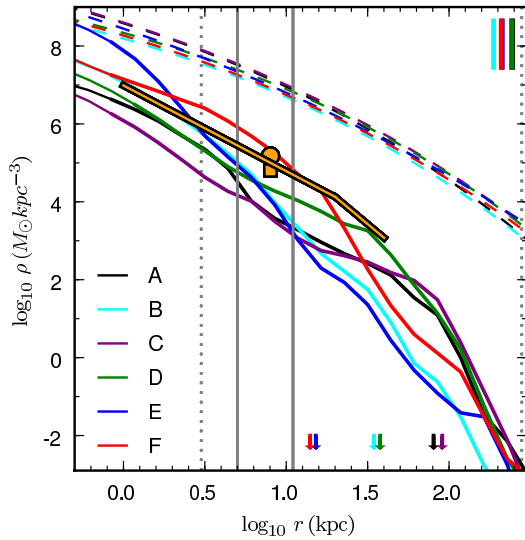


Fig. 6 From Cooper et al. (2010): Spherically averaged density profiles for the six Aquarius stellar haloes. Arrows mark the break radii of broken power-law fits to each profile. Dashed lines show Einasto profile fits to the corresponding dark matter haloes. Grey vertical lines demarcate what the authors define the ‘outer halo region’ (dotted) and the ‘solar neighbourhood’ (solid); coloured vertical bars indicate r_{200} for the dark haloes. Overplotted are representative data for the Milky Way (orange): estimates of the halo density in the solar neighbourhood (symbols) from Gould et al. (1998, square) and Fuchs & Jahreiß (1998, circle), and the best-fitting broken power law of Bell et al. (2008, excluding the Sagittarius stream and Virgo overdensity).

the inner regions of the stellar halo, however, their simulations tend to be significantly more clustered than the data. They argue that one possible explanation for this is the existence of a smooth component that is not currently included in their simulations, and that could originate from stars scattered from the disc or born on eccentric orbits. It would be interesting to improve the available models so as to include these physical processes.

5 The Milky Way satellites

As mentioned in Section 1, it has long been realized that the number and properties of the Milky Way satellites can be affected significantly by baryonic physics, in particular by reionization and supernovae feedback. Figs. 7 and 8 show the effect of these physical processes on the luminosity function of Milky-Way satellites, from two independently developed semi-analytic models both applied to the second highest level of resolution of the Aq-A halo.

Fig. 7 shows results from the model described in Font et al. (2011) who implemented a detailed treatment of reionization in the Durham semi-analytic model of galaxy formation, GALFORM. In this model, the UV flux produced by

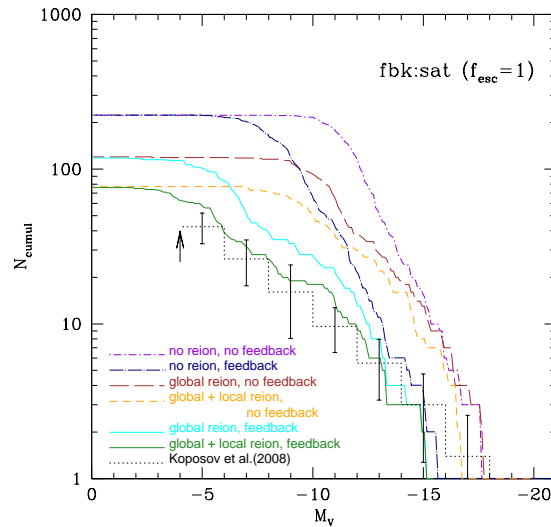


Fig. 7 From Font et al. (2011): The effect of different physical processes on the luminosity function of satellites in the Aq-A halo, in the fbk:sat model (see the original paper for details).

the galaxy population is calculated in a self-consistent way, and the contribution from quasars is taken from the observationally inferred spectrum of Haardt & Madau (1996). The model also allows for an additional local UV flux generated by the progenitors of the Milky Way galaxy. This results in an earlier effective redshift of reionization which suppresses the star formation in satellite galaxies, particularly in very low mass galaxies. In order to achieve a good agreement with observational measurements, the model requires, however, an escape fraction of UV photons of about 100 per cent. The figure shows that, in this model, the number of faint satellites is reduced by a combination of supernovae feedback and global+local photoheating. Supernovae feedback is effective in suppressing the more massive systems, while photoheating plays an important role in reducing the number of ultra-faint dwarfs. Local photoheating appears to be a crucial ingredient.

Fig. 8 shows the corresponding results from the model presented in Li et al. (2010), applied to the same dark matter simulation. This model is based on that described in De Lucia & Helmi (2008) but has been updated to provide a better match to the observed properties of Milky Way satellites. It differs from the model by Font et al. in a number of details. In particular: a simple reionization model, that does not account for local photoionization is adopted, based on the Gnedin (2000) formalism. Cooling via molecular hydrogen is not included, under the assumption that H_2 is efficiently photodissociated. All other physical processes considered are modelled using different prescriptions (see original papers for details). Fig. 8 shows that the relative importance of reionization and feedback is similar to that found in the Font et al. model: reionization alone is not able to

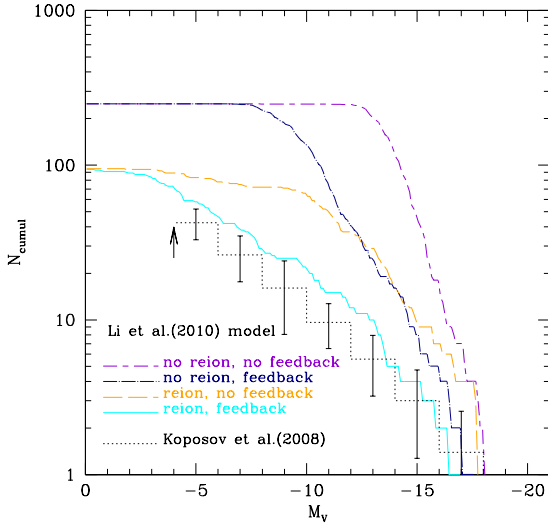


Fig. 8 From Font et al. (2011): Luminosity function for the Aq-A halo in the Li et al. (2010) model with global reionization and feedback switched on and off (see original papers for details).

bring the predicted number of luminous satellites in agreement with that observed, and is effective at the faint end of the luminosity function ($M_V \gtrsim -10$). Feedback from supernovae is instead important for more luminous satellites.

Similar conclusions have been reached also by Macciò et al. (2010) who compare results from three independently developed semi-analytic models of galaxy formation. The models are applied to high-resolution N -body simulations but do not use (as in the studies discussed above) the subhalo information to follow the evolution of the satellite population. Several other studies of the Milky Way satellites in a Λ CDM framework have been carried out recently. A brief overview of the most recent ones can be found in Appendix B of Font et al. (2011). Both Li et al. (2010) and Font et al. (2011) have compared predictions of their models with other physical properties of the Milky Way satellites. In particular, they have shown that both models are able to provide a relatively good agreement with the observed cumulative radial distribution of satellites and the observed metallicity-luminosity relation. Again, one important limitation of these studies is that they both assume an instantaneous recycling approximation for chemical enrichment.

The high resolution of the simulations used in the studies mentioned above allows the satellites dark matter mass enclosed within a (small) given radius to be measured. Fig. 9 shows how the mass within 600 pc ($M_{0.6}$) varies as a function of the V -band luminosity of model satellites in the top panel, and as a function of the total mass of the dark matter substructure in the bottom panel. Li et al. 2009 did not attempt to measure the mass within 300 pc (as done in more recent observational studies) as this would go beyond the resolution limit of the simulation used in their study (the

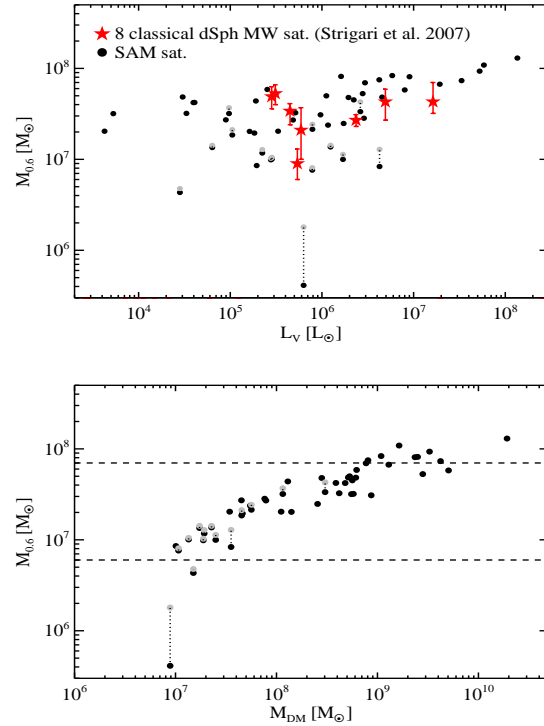


Fig. 9 From Li et al. (2009): The top panel shows the mass within 600 pc as a function of the V -band luminosity for model satellites, and for the eight brightest dwarf spheroidal galaxies of the Milky Way (asterisks). Black and grey circles corresponds to two alternative measurements of $M_{0.6}$ (see original paper for details). The bottom panel shows the mass within 600 pc as a function of the total mass of the dark matter substructure. The two dashed lines correspond to the upper and lower limits for the observational estimates by Strigari et al. 2008.

highest resolution simulation of the GA series). The figure shows that the correlation between $M_{0.6}$ and V -band luminosity is somewhat stronger than in the real data, but consistent with them. The bottom panel of Fig. 9 shows that the present day total mass of substructures hosting luminous satellites varies in the range $\sim 10^7$ - $10^{10} M_\odot$. The scatter reflects the lack of a tight concentration-virial mass relation, the different accretion times, and the different amounts of tidal stripping suffered by the parent substructures once they have fallen on to the Milky Way halo. Therefore, in the model by Li et al., a common mass scale within 600 pc for luminous satellites results from the strong suppression of accretion and cooling of gas in low mass haloes after reionization, as well as from the atomic hydrogen cooling threshold at $T_{\text{vir}} = 10^4$ K. Similar conclusions have been obtained in more recent studies that have taken advantage of higher resolution simulations to measure the mass within a radius of 300 pc. Interestingly, all these studies have found a weak dependence of M_{300} on luminosity (e.g. Macciò et al. 2009, Muñoz et al. 2009, Busha et al. 2010, Font et al.

2011). This represents then a robust and testable prediction that requires improved measurements of M_{300} .

6 Things we have learned

The work discussed above has demonstrated that, within the current standard paradigm for structure formation, it is possible to reproduce the basic properties of our Milky Way and of its satellite systems using *plausible* prescriptions to model the relevant physical processes at play.

In agreement with earlier studies, recent work has confirmed that combining a sufficiently high redshift of reionization with a relatively strong feedback from supernovae, it is possible to bring the predicted number of luminous satellites in agreement with the most recent observational results. The same models provide a relatively good agreement with some basic physical properties measured for the Milky Way satellites. In addition, the models also provide an explanation for the apparent common mass scale of dwarf galaxies, which results from a weak dependence of M_{300} on the virial mass of the substructures hosting luminous galaxies. In fact, models predict a weak increase of M_{300} for increasing luminosity which will be testable once more accurate measurements are available.

Model results depend strongly on the particular implementation of supernovae feedback, which is effective in suppressing the formation of relatively luminous satellites. A scheme which is more efficient in galaxies residing in lower mass haloes provides, however, a better agreement with the properties of the ultra-faint satellites. In the framework of these models, the brightest satellites are associated with the most massive subhaloes and are accreted relatively recently ($z < 1$). They have extended star formation histories and only a small fraction of their stars are made by the end of the reionization. On the other hand, fainter satellites tend to be accreted early, are dominated by old stellar populations, and a number of them formed most of their stars before reionization was complete.

The stellar halo is built predominantly by accretion of satellites at early times. A range of accretion histories is possible, from smooth growth of the stellar halo to growth in one or two discrete events. The most significant accretion events are those that occurred more recently, and they dominate the stellar halo at large radii. The halo has a complex structure, with well-mixed components, tidal streams, and shells, that is not well described by smooth models.

In these models, the stars in the halo do not exhibit any significant metallicity gradient, but higher metallicity stars are more centrally concentrated than stars with lower abundances.

This is due to the fact that the most massive satellites contributing to the stellar halo are also the most metal rich, and dynamical friction drags them closer to the inner regions of the host halo. Finally, in the context of these models, the observed abundance pattern of the stellar halo and of the surviving dwarf spheroidals can be reproduced.

7 Open issues

However, we are not left without problems, and open questions.

Most of the recently published hybrid models (including all those discussed in the previous sections) adopt an instantaneous recycling approximation which is inappropriate for the iron-peak elements, mainly produced by supernovae Type Ia. This is a crucial missing ingredient in order to understand if the models discussed above are really successful (see e.g. discussion related to Fig. 3). Work is ongoing in order to improve the available models by taking into account time-dependent yields and following explicitly the evolution of different elements. This will allow a more direct and thorough comparison with available observational data to be carried out, thereby providing even stronger constraints on available models.

At least for some of the models discussed above, the predicted relation between stellar mass and dark matter mass (at the time of infall for satellite galaxies) is offset with respect to that obtained using abundance matching techniques (Guo et al. 2010). This goes in the sense that at a given luminosity, model galaxies reside in smaller dark matter haloes. The difference is largest at small masses where observational constraints are poor, but it persists also at scales of the Milky Way galaxy (Starkenburg et al., in preparation). Guo et al. (2011) have recently presented an extension of previous models that shows a good agreement with the relation derived from abundance matching. In order to achieve this match, the model adopts a supernovae feedback ejection efficiency that depends strongly on the velocity of the parent dark matter halo. The predicted luminosity function of Milky Way satellites is marginally inconsistent with the observed number of faint satellites, although still plausible given the observational uncertainties. It will be interesting to check if this model also reproduces the detailed physical and chemical properties of the Milky Way satellite galaxies.

Recently, Boylan-Kolchin et al. (2011a) have shown that the state-of-the-art collisionless N -body simulations predict a population of massive dark matter substructures that are too concentrated (have too high a V_{\max} for a given r_{\max}) to be able to host the brightest satellites of the Milky Way. The problem is illustrated in Fig. 10 that shows the location in the V_{\max} versus r_{\max} plane for subhaloes extracted from the six Aquarius haloes and from the via Lactea II simulation, and the constraints from the Milky Way dwarf spheroidal galaxies. This poses a problems for abundance matching methods that, while reproducing the luminosity function of the Milky Way satellites, they do so by assigning the brightest satellites to haloes that are denser than observed. In a follow-up paper, Boylan-Kolchin et al. (2011b) have explored possible solutions to these problems, in the context of Λ CDM and argued that all of them appear to be unlikely. In particular, they have analysed the following options: (1) an atypical Milky Way halo that is either deficient in massive subhaloes or populated by atypical substructures;

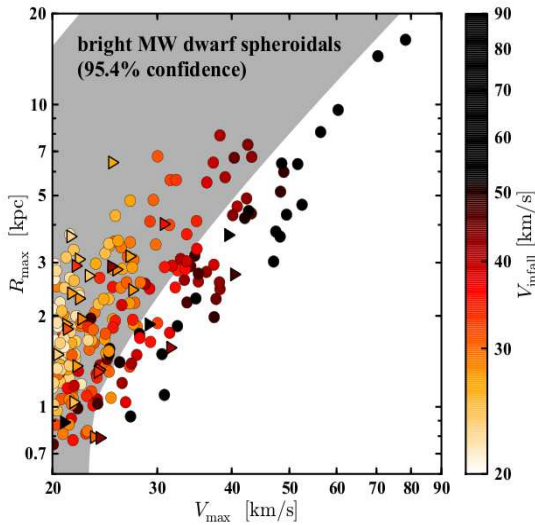


Fig. 10 From Boylan-Kolchin et al. (2011a): subhaloes from all six Aquarius simulations (circles) and from the Via Lactea II simulation (triangles), colour-coded according to V_{infall} . The grey-shaded region shows the 2σ confidence interval for possible hosts of the bright Milky Way dwarf spheroidals (see original paper for details).

(2) a stochastic galaxy formation at small scales that washes out the correlation between halo mass and luminosity; (3) strong baryonic feedback that reduces the central density of massive subhaloes by large amounts. If all of the ‘astrophysical solutions’ are rejected, we are left with the more fundamental problem of the nature of dark matter. For example, in a very recent work, Lovell et al. (2011) argue that no such problem exists if haloes are made of warm dark matter.

Finally, it remains to be verified that a good agreement with the number and also the physical properties of the dwarf satellites of the Milky Way can be retained while simultaneously matching the properties of the global galaxy population at different cosmic epochs.

Acknowledgements. I thank the organizers of the AG2011 meeting for the invitation, and for the friendly and stimulating atmosphere. I acknowledge financial support from the European Research Council under the European Community’s Seventh Framework Programme (FP7/2007-2013)/ERC grant agreement n. 202781.

References

Bell, E. F. et al.: 2008, *ApJ* 680, 295
 Benson, A.J., Frenk, C.S., Lacey, C.G., Baugh, C.M., Cole, S.: 2002, *MNRAS* 333, 177
 Benson, A.J., Bower, R.: 2010, *MNRAS* 405, 1573
 Boylan-Kolchin, M., Bullock, J.S., Kaplinghat, M.: 2011a, *MNRAS* 415, L40
 Boylan-Kolchin, M., Bullock, J.S., Kaplinghat, M.: 2011b, *MNRAS* submitted, arXiv:1111.2048
 Bullock, J.S., Kravtsov, A.V., Weinberg, D.H.: 2000, *ApJ* 539, 517

Bullock, J.S., Johnston, K.V.: 2005, *ApJ* 635, 931
 Busha, M.T., Alvarez, M.A., Wechsler, R.H., Abel, T., Strigari, L.E.: 2010, *ApJ* 710, 408
 Carollo, D. et al.: 2007, *Nature* 450, 1020
 Cooper, A.P., Cole, C., Frenk, C.S., White, S.D.M., Helly, J., Benson, A.J., De Lucia, G., Helmi, A., Jenkins, A., Navarro, J.F., Springel, V., Wang, J.: 2010, *MNRAS* 406, 744
 Cooper, A.P., Cole, S., Frenk, C.S., Helmi, A.: 2011, *MNRAS* 417, 2206
 De Lucia, G., Blaizot, J.: 2007, *MNRAS* 375, 2
 De Lucia, G., Helmi, A.: 2008, *MNRAS* 391, 14
 Diemand, J. et al.: 2008, *Nature* 454, 735
 Efstathiou G.: 1992, *MNRAS* 256, 43
 Eggen, O.J., Lynden-Bell, D., Sandage, A.R.: 1962, *ApJ* 136, 748
 Font, A.S., Johnston, K.V., Bullock, J.S., Robertson, B.E.: 2006, *ApJ* 638, 585
 Frebel, A., Kirby, E.N., Simon, J.D.: 2010, *Nature* 464, 72
 Fuchs, B., Jahreiß, H.: 1998, *A&A* 329, 81
 Gnedin, N.Y.: 2000, *ApJ* 542, 535
 Gould, A., Flynn, C., Bahcall, J.N.: 1998, *ApJ* 503, 798
 Guo, Q., White, S.D.M., Li, C., Boylan-Kolchin, M.: 2010, *MNRAS* 404, 1111
 Guo, Q., White, S.D.M., Boylan-Kolchin, M., De Lucia, G., Kauffmann, G., Lemson, G., Li, C., Springel, V., Weinmann, S.: 2011, *MNRAS* 413, 101
 Haardt, F., Madau, P.: 1996, *ApJ* 461, 20
 Helmi, A.: 2008, *Astronomy and Astrophysics Review* 15, 145
 Helmi, A., Navarro, J.F., Nordström, B., Holmberg, J., Abadi, M.G., Steinmetz, M.: 2006, *MNRAS* 365, 1309
 Kauffmann, G., White, S.D.M., Guiderdoni, B.: 1993, *MNRAS* 264, 201
 Kirby, E.N., Simon, J.D., Geha, M., Guhathakurta, P., Frebel, A.: 2008, *ApJ* 685, 43
 Klypin, A., Kravtsov, A.V., Valenzuela, O., Prada, F.: 1999, *ApJ* 522, 82
 Li, Y.-S., Helmi, A., De Lucia, G., Stoehr, F.: 2009, *MNRAS* 397, 87
 Lovell, M., Eke, V., Frenk, C., Gao, L., Jenkins, A., Theuns, T., Wang, J., White, S., Boyarsky, A., Ruchayskiy, O.: 2011, *MNRAS* in press, arXiv:1104.2929
 Matteucci, F.: 2008, *Proceedings of the 37th Saas-Fee Advanced Course of the Swiss Society for Astrophysics and Astronomy*, arXiv:0804.1492
 Macciò, A.V., Kang, X., Moore, B.: 2009, *ApJ* 692, 109
 Macciò, A.V., Kang, X., Fontanot, F., Somerville, R.S., Kopusov, S., Monaco, P.: 2010, *MNRAS* 402, 1995
 Monaco, P., Fontanot, F., Taffoni, G.: 2007, *MNRAS* 375, 1189
 Moore, B., Ghigna, S., Governato, F., Lake, G., Quinn, T., Stadel, J., Tozzi, P.: 1999, *ApJ* 524, L19
 Muñoz, J.A., Madau, P., Loeb, A., Diemand, J.: 2009, *MNRAS* 400, 1593
 Nordström, B., Mayor, M., Andersen, J., Holmberg, J., Pont, F., Jørgensen, B.R., Olsen, E.H., Udry, S., Mowlavi, N.: 2004, *A&A* 418, 989
 Okamoto, T., Gao, L., Theuns, T.: 2008, *MNRAS* 390, 920
 Scannapieco, C., et al.: 2011, *MNRAS* submitted, arXiv:1112.0315v1
 Searle, L., Zinn, R.: 1978, *ApJ* 225, 357
 Shetrone, M.D., Cote, P., Sargent, W.L.W.: 2001, *ApJ* 548, 592
 Somerville, R.S., Hopkins, P.F., Cox, T.J., Robertson, B.E., Hernquist, L.: 2008, *MNRAS* 391, 481
 Springel, V., Wang, J., Vogelsberger, M., Ludlow, A., Jenkins, A., Helmi, A., Navarro, J.F., Frenk, C.S., White, S.D.M.: 2008,

- MNRAS 391, 1685
Stoehr, F., White, S.D.M., Springel, V., Tormen, G., Yoshida, N.:
2003, MNRAS 345, 1313
Strigari, L.E., Bullock, J.S., Kaplinghat, M., Simon, J.D., Geha,
M., Willman, B., Walker, M.G.: 2008, Nature 454, 1096
White, S.D.M., Rees, M.J.: 1978, MNRAS 183, 341
Wyse, R.F.G., Gilmore, G.: 1995, AJ 110, 2771
Zoccali, M., Renzini, A., Ortolani, S., Greggio, L., Saviane, I.,
Cassisi, S., Rejkuba, M., Barbuy, B., Rich, R.M., Bica, E.:
2003, A&A 399, 931
Zoccali, M., Hill, V., Lecureur, A., Barbuy, B., Renzini, A., Min-
niti, D., Gómez, A., Ortolani, S.: 2008, A&A 486, 177